EARTHQUAKE ENGINEERING AND STRUCTURAL DYNAMICS, VOL. 26, 951–965 (1997)

SENSITIVITY ANALYSIS ON MEASUREMENT NOISE IN THE IDENTIFICATION OF SOIL PROPERTIES FROM VERTICAL ARRAY OBSERVATION DATA

TETSUSHI KURITA[1]* AND KUNIHITO MATSUI[2]

[1]*Seismic Engineering Department, Tokyo Electric Power Services Co., Ltd., 3-3-3, Higashi-Ueno, Taito-ku, Tokyo 110, Japan*
[2]*Department of Civil Engineering, Tokyo Denki University, Hatoyama, Hiki, Saitama 350-03, Japan*

SUMMARY

This study clarified the effects of measurement noise on identification of soil properties from vertical array observation of seismic waves. In order to evaluate the sensitivity of the unknown parameter with respect to error caused by noise, the amplitude of a transfer function was used to formulate the evaluation function in the frequency domain. Also the logarithmic amplitude was used to formulate the evaluation function and compare the sensitivity between the two types of amplitude expressions. A numerical experiment, based on a simple-structured ground model, showed that these evaluation functions produced satisfactory results which were in good agreement with identified results obtained by the measurement data contaminated by artificially generated errors. The present theory, when applied to actual earthquake records, proved useful in evaluating the influence of the non-linearity of soil characteristics. © 1997 by John Wiley & Sons, Ltd.

Earthquake Engng. Struct. Dyn., **26**, 951–965 (1997)

No. of Figures: 8. No. of Tables: 10. No. of References: 17.

KEY WORDS: parameter identification; sensitivity analysis; measurement noise; vertical array observation; S-wave velocity; damping factor

1. INTRODUCTION

An increasing number of vertical array systems are being installed in the ground. Seismic data obtained by these vertical arrays has been applied to identify the velocity and damping in the layered soil deposits.[1–6] Depending on how the data is handled, there are two types of dynamic identification available: one is made in the time domain,[6] the other in the frequency domain.[7,8] The frequency-domain identification is more favourable when a fairly large amount of measurement data is available. This is partly because a geometric mean of the Fourier spectral ratio may be employed to estimate the average soil properties of the ground. This type of identification is particularly useful when the transfer function differs from one seismic measurement to another.

The authors[9,10] have proposed a method of identifying the structural parameters in the time domain by the Gauss–Newton method, and examined its usefulness by simulation. The authors have also studied the effects of errors in model parameters and measurement noise on identified results in the time domain.[11] The sensitivity of an unknown parameter with respect to errors and noise may help determine both the reliability of identification and the required accuracy of the parameter. It may also provide useful information about the optimal arrangement of measurement devices.[12] Thus, it is important to evaluate the effects of the model

* Correspondence to: T. Kurita, Seismic Engineering Department, Tokyo Electric Power Services Co., Ltd. 3-3-3, Higashi-Ueno, Taito-ku, Tokyo 110, Japan. E-mail: kurita@aed.tepsco.jp

CCC 0098–8847/97/090951–15$17·50

Received 17 October 1995
Revised 2 January 1997

parameter errors and measurement noises on identification problems. However, few researchers have discussed these points of view. Tsujihara *et al.*[13] added noise during measurement to compare the influence of errors between various methods of identification. Yoshida *et al.*[14] studied the standard deviation of measurement error and the accuracy of identified results in static identification problems.

The present study followed the idea given in Reference 11 to derive an equation of sensitivity of unknown parameters with respect to measurement noise when identifying the dynamic properties of the soil deposits. Then this equation was applied to actual earthquake records obtained from a vertical array system.

The effect of error in identification problems is investigated in this research. Two types of error effects are considered. One is an effect of model parameter error and the other is that of measurement noise. The seismic ground motion of near-surface sedimentary ground is, in general, expressed by one-dimensional layer model. This paper focuses on the latter effect. Sensitivity formula of unknown parameters with respect to measurement noise is derived. The sensitivity expresses the rate of change in the parameter values due to the noise. If the sensitivities are large, it implies that the identified results might be greatly effected by measurement noise. If this is the case, accuracy in measurement has to be improved to obtain reliable results. Considering that the sensitivity depends on sensor location, the information can be employed for determination of the sensor allocation that produces smaller noise effect on identified results.

2. EVALUATION FUNCTION FOR IDENTIFICATION PROBLEM IN THE FREQUENCY DOMAIN

Horizontally layered soil deposits subjected to an earthquake are digitized as an assembly of one-dimensional shear beam elements. The equation of motion for this linear multi-freedom system can be expressed as follows:

$$\mathbf{M}\ddot{\mathbf{z}}(t) + \mathbf{K}^*\mathbf{z}(t) = -\mathbf{M}\mathbf{1}\ddot{y}_0(t) \tag{1}$$

where $\mathbf{M}$ and $\mathbf{K}^*$ are the consistent mass matrix and complex stiffness matrix, $\ddot{\mathbf{z}}(t)$ and $\mathbf{z}(t)$ are the acceleration vector and displacement vector relative to the base layer. $\mathbf{1}$ is a vector whose all entities are 1, $\ddot{y}_0(t)$ is a scalar quantity representing the earthquake motion (acceleration) of the base layer. Equation (1) represents hysteretic damping due to complex stiffness. The complex stiffness of each element is given by

$$k_j^* = k_j(1 + 2h_j i) \quad (j = 1, \ldots, K) \tag{2}$$

where k_j is the elemental stiffness, h_j is the damping factor, i is the imaginary unit and K stands for the degree of freedom. The complex response analysis method was applied to formulate an evaluation function for identification in the frequency domain. A Fourier transform of both sides of equation (1) yields

$$(-\omega^2\mathbf{M} + \mathbf{K}^*)\mathbf{U}(\omega) = \omega^2\mathbf{M}\mathbf{1}Y_0(\omega) \tag{3}$$

where $\mathbf{U}(\omega)$ is the Fourier transform of the relative displacement, $\mathbf{z}(t)$, and $Y_0(\omega)$ is the Fourier transform of the base layer displacement, $y_0(t)$. Equation (3) yields a transfer function for each nodal point, with respect to the base layer, as follows:

$$\mathbf{H}(\omega) = \omega^2(-\omega^2\mathbf{M} + \mathbf{K}^*)^{-1}\mathbf{M}\mathbf{1} + \mathbf{1} \tag{4}$$

Equation (4) was used to generate an evaluation function. Since $\mathbf{H}(\omega)$ is complex, its absolute value of amplitude is often used. As a Fourier transform pair of the transfer function in the frequency domain, the impulsive response function in the time domain is the minimum phase transition function. Therefore, a Hilbert transform of the transfer function's amplitude may define the phase angle completely. As Sawada *et al.*[7] indicated, a structural identification may be obtained solely from the amplitude of a transfer function. This is particularly useful when using earthquake records. In this case, the phase angle of the transfer function calculated from observation data is not accurate enough, but generation of an evaluation function from the amplitude is practical.

Let $\mathbf{X} = \{X_1, X_2, \ldots, X_M\}$ represent a set of unknown parameters and $\mathbf{Y} = \{Y_1, Y_2, \ldots, Y_L\}$ represent a set of known constants. By employing the concept of the least-squares method, the evaluation function may be defined as

$$J(\mathbf{X}, \mathbf{Y}) = \frac{1}{2} \sum_{m=1}^{N} \left[\sum_{i \in A} w_i \{ |R_i(\omega_m)| - |H_i(\omega_m)| \}^2 \right] \tag{5}$$

where $R_i(\omega_m)$, $(i \in A)$ is the Fourier spectral ratio of measured data. Here, A represents a set of spectral ratio combinations. w_i is the weight coefficient, which may vary depending on the importance and reliability of the measurements.[15] It may be noted that the transfer function is digitized like ω_m, $(m = 1, \ldots, N)$ on the circular frequency axis. The use of a natural logarithmic Fourier spectral ratio (transfer function) may allow an evaluation function of the following form:[1]

$$J(\mathbf{X}, \mathbf{Y}) = \frac{1}{2} \sum_{m=1}^{N} \left[\sum_{i \in A} w_i \{ \ln|R_i(\omega_m)| - \ln|H_i(\omega_m)| \}^2 \right] \tag{6}$$

The evaluation function of equation (5) places stress on the remainder near the peak of amplitude. One the other hand, equation (6) tends to equally evaluate both the peaks and troughs of the transfer function. These two equations are used to examine the effects of measurement noise. The evaluation functions, equations (5) and (6), are called Type 1 and Type 2 functions, respectively. Let $\bar{\mathbf{Y}}$ be the true value of a constant vector $\mathbf{Y}$ and $\overline{R_i(\omega_m)}$ be the remainder of the Fourier spectral ratio after measurement noise is removed. Then, $\partial J / \partial X_j = 0$, $(j = 1, \ldots, M)$ is the condition of minimizing the evaluation function of equations (5) and (6) as well. Let $\bar{\mathbf{X}}$ represent the value of $\mathbf{X}$ that meets this condition. In this case, $J_{\min}$ is zero. Thus, equations (5) and (6) become

$$J_{\min} = J(\bar{\mathbf{X}}, \bar{\mathbf{Y}}) = \frac{1}{2} \sum_{m=1}^{N} \left[\sum_{i \in A} w_i \{ |\overline{R_i(\omega_m)}| - |H_i(\omega_m)| \}^2 \right] = 0 \tag{7}$$

$$J_{\min} = J(\bar{\mathbf{X}}, \bar{\mathbf{Y}}) = \frac{1}{2} \sum_{m=1}^{N} \left[\sum_{i \in A} w_i \{ \ln|\overline{R_i(\omega_m)}| - \ln|H_i(\omega_m)| \}^2 \right] = 0 \tag{8}$$

Identified results form uncontaminated data are considered as true values. However, since in a real world the true values of model parameters are not known, identified values are good approximation to the true values. In this minimization process, the partial differentiation coefficients of an unknown parameter took the following form:

$$\frac{\partial |\mathbf{H}(\omega)|}{\partial X_j} = \frac{1}{2} \left\{ \frac{\partial \mathbf{H}(\omega)}{\partial X_j} \mathbf{H}^*(\omega) + \mathbf{H}(\omega) \frac{\partial \mathbf{H}^*(\omega)}{\partial X_j} \right\} \{ \mathbf{H}(\omega) \mathbf{H}^*(\omega) \}^{-1/2} \quad (j = 1, \ldots, M) \tag{9}$$

where the suffix $(\cdot)^*$ indicates a conjugate complex number. Similarly, the partial differentiation coefficients of an unknown parameter in natural logarithmic form took the following form:

$$\frac{\partial \ln|\mathbf{H}(\omega)|}{\partial X_j} = |\mathbf{H}(\omega)|^{-1} \frac{\partial |\mathbf{H}(\omega)|}{\partial X_j} \quad (j = 1, \ldots, M) \tag{10}$$

3. EFFECTS OF MEASUREMENT NOISE CONTAINED IN THE RESPONSE

3.1. Derivation of formulas

It was first assumed that the measured values contain noise in the measurement at one sensor location ℓ but no noise in the measurements $|\overline{R_i(\omega_m)}|$, $(i \in A, i \neq \ell)$ at the other locations. It was also assumed that the

parameter $\mathbf{Y}$ of the structural model contains no error. Let $|\overline{R_\ell(\omega_m)}|$ represent the true value of a measured value $|R_\ell(\omega_m)|$ at the location ℓ and $|R_\ell(\omega_m)| = |\overline{R_\ell(\omega_m)}| + \Delta R_\ell(\omega_m)$ represent the measured value containing noise. Then, $\Delta R_\ell(\omega_m) = \varepsilon_\ell \eta_\ell(\omega_m)$, where $\eta_\ell(\omega_m)$ is a normalized error vector and ε_ℓ is a scalar representing the magnitude of the error. It is assumed that measurement noise at each sensor is independent. In this case, the unknown parameter $\mathbf{X}$ may be expressed by $\bar{\mathbf{X}} + \Delta\mathbf{X}^{(\ell)}$. $\Delta\mathbf{X}^{(\ell)}$ is the difference from the true value, caused by measurement error $\Delta R_\ell(\omega_m)$. The evaluation function now becomes

$$J = \frac{1}{2}\sum_{m=1}^{N}\left[\sum_{\substack{i\in A\\ i\neq\ell}} w_i\{|\overline{R_i(\omega_m)}| - |H_i(\omega_m, \bar{\mathbf{X}} + \Delta\mathbf{X}^{(\ell)})|\}^2 + w_\ell\{|\overline{R_\ell(\omega_m)}| + \Delta R_\ell(\omega_m) - |H_\ell(\omega_m, \bar{\mathbf{X}} + \Delta\mathbf{X}^{(\ell)})|\}^2\right] \tag{11}$$

Assuming that the measurement error, $\Delta R_\ell(\omega_m) = \varepsilon_\ell \eta_\ell(\omega_m)$, is small enough to have insignificant influence on the identification, the following approximate value of amplitude may be obtained:

$$\begin{aligned} |H_i(\omega_m, \bar{\mathbf{X}} + \Delta\mathbf{X}^{(\ell)})| &= |H_i(\omega_m, \bar{\mathbf{X}})| + \sum_{j=1}^{M}\frac{\partial|H_i(\omega_m)|}{\partial X_j}\frac{\partial X_j}{\partial R_\ell}\Delta R_\ell(\omega_m) \\ &= |H_i(\omega_m, \bar{\mathbf{X}})| + \sum_{j=1}^{M}\frac{\partial|H_i(\omega_m)|}{\partial X_j}\frac{\partial X_j}{\partial \varepsilon_\ell}\frac{\partial \varepsilon_\ell}{\partial R_\ell}\Delta R_\ell(\omega_m) \\ &= |H_i(\omega_m, \bar{\mathbf{X}})| + \sum_{j=1}^{M}\frac{\partial|H_i(\omega_m)|}{\partial X_j}\Gamma_{j\ell}\varepsilon_\ell \end{aligned} \tag{12}$$

where $\Gamma_{j\ell} = \partial X_j/\partial\varepsilon_\ell$. Substituting equation (12) into equation (11) and noting the relation of $|\overline{R_i(\omega_m)}| = |H_i(\omega_m, \bar{\mathbf{X}})|$, equation (11) can be rewritten as

$$J = \frac{\varepsilon_\ell^2}{2}\sum_{m=1}^{N}\left[\sum_{\substack{i\in A\\ i\neq\ell}} w_i\left\{-\sum_{j=1}^{M}\frac{\partial|H_i(\omega_m)|}{\partial X_j}\Gamma_{j\ell}\right\}^2\right] + \frac{\varepsilon_\ell^2}{2}\sum_{m=1}^{N}\left[w_\ell\left\{-\sum_{j=1}^{M}\frac{\partial|H_\ell(\omega_m)|}{\partial X_j}\Gamma_{j\ell} + \eta_\ell(\omega_m)\right\}^2\right] \tag{13}$$

Applying the necessary condition of $\partial J/\partial\Gamma_{k\ell} = 0$ for equation (13) to minimize regardless of the value of ε_ℓ^2, with respect to the unknown parameter $\Gamma_{j\ell}$, the sensitivity equation is the following:

$$\sum_{j=1}^{M}\left\{\sum_{m=1}^{N}\sum_{i\in A} w_i\frac{\partial|H_i(\omega_m)|}{\partial X_j}\frac{\partial|H_i(\omega_m)|}{\partial X_k}\right\}\Gamma_{j\ell} = \sum_{m=1}^{N} w_\ell\eta_\ell(\omega_m)\frac{\partial|H_\ell(\omega_m)|}{\partial X_k} \quad (k = 1, \ldots, M) \tag{14}$$

Here, $\Gamma_{j\ell}$ gives the sensitivity of the unknown parameter with respect to measurement noise. Similarly, for an evaluation function of natural logarithmic amplitude, the sensitivity equation becomes

$$\sum_{j=1}^{M}\left\{\sum_{m=1}^{N}\sum_{i\in A} w_i\frac{\partial\ln|H_i(\omega_m)|}{\partial X_j}\frac{\partial\ln|H_i(\omega_m)|}{\partial X_k}\right\}\Gamma_{j\ell} = \sum_{m=1}^{N} w_\ell\eta_\ell(\omega_m)\frac{\partial\ln|H_\ell(\omega_m)|}{\partial X_k} \quad (k = 1, \ldots, M) \tag{15}$$

3.2. *Numerical example*

To verify proposed theory, a numerical simulation is performed using the two-layer soil deposits model shown in Figure 1. There were two seismometers in the vertical array system: one on the ground level (GL. 0 m) and another on the base layer (GL. −30 m). Figure 2 shows the amplitude, with respect to the base layer, of the ground-level transfer function. Each layer was divided into five sub-layer elements, as shown in Figure 1. This was a condition for possible propagation of a wave having the shortest wavelength within the

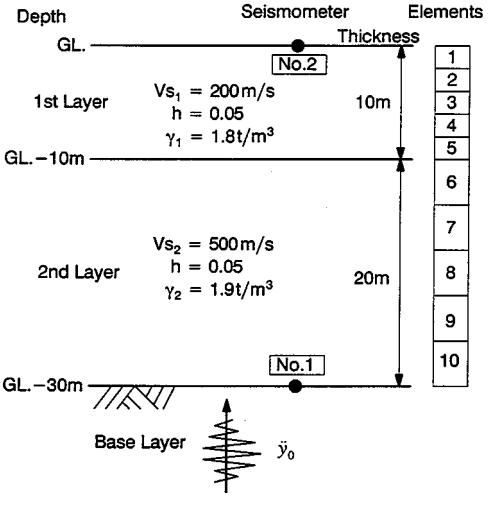

Figure 1. Two-layer model

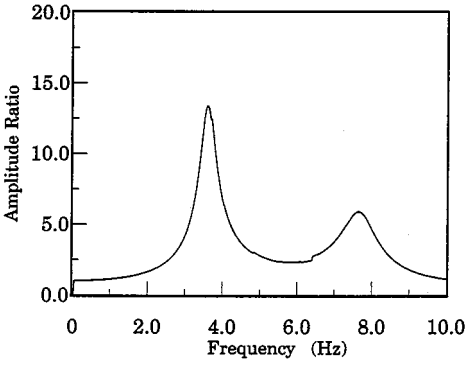

Figure 2. Amplitude ratio of transfer function

frequency range under consideration. The input wave in the base layer was a modification of the El Centro wave (NS component) in the 1940 Imperial Valley Earthquake, with the maximum acceleration adjusted to 100 gal. The seismic response at the seismometer location was obtained by the complex response analysis method using the transfer function equation (4). Then, band-limited white noise of 5, 10, or 20 per cent in magnitude in a range of frequencies from 0·02 to 25 Hz was added to the seismic response to obtain a simulation of the measured data. The magnitude of additional noise is the percentage of the largest waveform of noise compared to the maximum acceleration of a response waveform.

Figure 3 shows a Fourier spectrum for the acceleration response with 20 per cent noise added at the ground level (GL. 0 m). This figure clearly shows that the signal was hidden behind noise except for the band-width between 0·3 and 10 Hz. Therefore, the range of frequencies between 0·3 and 10 Hz was selected for later analyses. Figure 4 shows a Fourier spectral ratio with respect to the response waveform with 20 per cent noise added at the ground-level measurement. In this figure, there was no noise added to the input waveform. Figure 5 shows the difference from the true value of this spectral ratio, or difference $\Delta R_\ell(\omega_m)$.

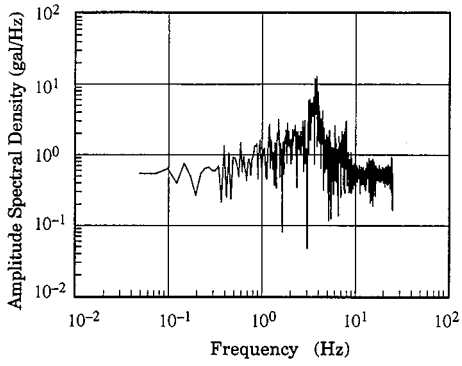

Figure 3. Fourier spectrum

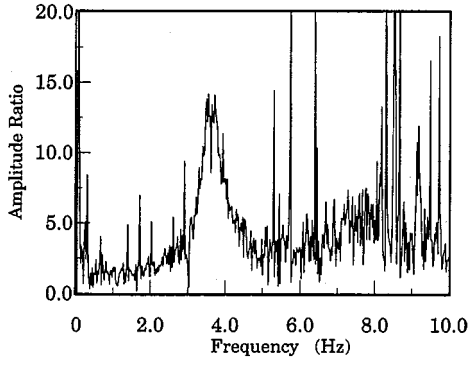

Figure 4. Fourier spectral ratio with respect to the response waveform with 20 per cent noise added

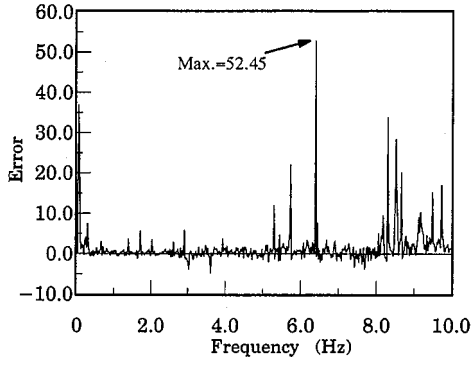

Figure 5. Error of Fourier spectral ratio with respect to the response waveform with 20 per cent noise added

Suppose the only unknown parameters are the S-wave velocity of each layer and the common damping factor for all the layers. In the following analysis, the weight coefficient was set to 1. Table I shows the sensitivities of these parameters with respect to measurement noise. In this calculation, equation (14) was used. The evaluation function was Type 1. Each value given in this table shows fluctuation from the true

Table I. Sensitivities of unknown parameters with respect to measurement noise (Type 1 function)

Noise (%)	ε_1	$\frac{\partial h}{\partial \varepsilon_1}$	$\frac{\partial Vs_1}{\partial \varepsilon_1}$	$\frac{\partial Vs_2}{\partial \varepsilon_1}$
5	9·23151	$0{\cdot}93436 \times 10^{-3}$	$0{\cdot}67657 \times 10^{-1}$	$0{\cdot}10991 \times 10^{0}$
10	23·6368	$0{\cdot}33575 \times 10^{-3}$	$0{\cdot}89964 \times 10^{-1}$	0.90255×10^{-1}
20	52·4558	$0{\cdot}10111 \times 10^{-3}$	$0{\cdot}11805 \times 10^{0}$	$0{\cdot}83824 \times 10^{-1}$

Units $\partial h/\partial \varepsilon_1$: no dimension, $\partial Vs_i/\partial \varepsilon_1$: (m/s)

value when the observation errors were normalized (i.e., the maximum is 1). Therefore, the product of each listed value and corresponding actual error magnitude gives the fluctuation from true value. Table I shows that the observation error had only a very small effect on the identified parameters. In particular, the S-wave velocity was nearly insensitive to observation error.

To test the accuracy of the sensitivities given in Table I, comparisons were made between the results obtained by using the value estimated from the sensitivities $(\bar{\mathbf{X}} + (\partial \mathbf{X}/\partial \varepsilon_\ell)\varepsilon_\ell)$ and the identified results calculated from the measurement data containing noise. The modified Marquardt method[16] was used for this identification analysis. Table II shows the results of this comparison. The converged values were obtained when the evaluation function was at its smallest values. First iterative values were the first values in the iteration calculation. In Table II, the estimated values from the sensitivities are in good agreement with the first iterative values. As the SN ratio and noise became larger, the estimated values deviated even more from the converged values. This is presumably because the identified values do not have a linear relationship with the measurement noises. Table II shows that the estimated damping factors from the sensitivities agreed well with the convergent values. For the S-wave velocity, agreement between the estimated and convergent values got worse as the errors increased. In the case of 20 per cent noise, agreement was very poor. A plausible reason for this is that the actual errors went beyond the small limit of errors that was assumed for the present theory.

Table III shows those sensitivities of the parameters to measurement errors that were obtained by using the Type 2 sensitivity function of equation (15). The sensitivities in this table are larger than those given in Table I for a Type 1 function. This is presumably because the Type 2 function might evaluate the transfer function equally both at troughs and at peaks, while the Type 1 function might underestimate it at the trough. Table IV shows a comparison of the estimated values from sensitivities and the identified values. A comparison of this table with Table II reveals that for the Type 2 function, observation error had a larger effect on identified results than for the Type 1 function. The Type 2 function gave better agreement between the estimated and identified results. This function also estimated values almost identical to the first iterative value and converged value. One reason for this may be that the maximum value of errors for 20 per cent noise was 52·5 in the case of the Type 1 function, which is larger than the prescribed range of theoretical errors, while it was 3·0 in the case of the Type 2 function.

4. APPLICATION TO ACTUAL EARTHQUAKE RECORDS

In this section, the earthquake records obtained from the dense vertical array system installed at Chiba Experiment Station, Institute of Industrial Science, University of Tokyo, was used for the measurement data.[17] A PS logging of the soil at this location clarified the S and P wave velocity. The Chibaken–Toho-Oki earthquake, which occurred on December 17, 1987, and the succeeding five aftershocks, were selected for the demonstration. Table V shows the basic information on these earthquakes. Each seismometer had three axial

Table II. Estimates from the sensitivities and the identified results (Type 1 function)

	Noise: 5%			Noise: 10%			Noise: 20%		
		Identified			Identified			Identified	
Parameter	Estimated	1st iterative value	Converged value	Estimated	1st iterative value	Converged value	Estimated	1st iterative value	Converged value
h	0·0586	0·0586	0·0585	0·0579	0·0579	0·0569	0·0553	0·0553	0·0501
Vs_1 (m/s)	200·62	200·62	200·84	202·13	202·13	208·26	206·19	206·19	223·94
Vs_2 (m/s)	501·01	501·01	501·17	502·13	502·13	498·20	504·40	504·40	498·35

Table III. Sensitivities of unknown parameters with respect to measurement noise (Type 2 function)

Noise (%)	ε_1	$\frac{\partial h}{\partial \varepsilon_1}$	$\frac{\partial Vs_1}{\partial \varepsilon_1}$	$\frac{\partial Vs_2}{\partial \varepsilon_1}$
5	2·81886	$0{\cdot}36729 \times 10^{-2}$	$0{\cdot}46954 \times 10^{0}$	$0{\cdot}10509 \times 10^{1}$
10	2·25321	$0{\cdot}34843 \times 10^{-2}$	$0{\cdot}25041 \times 10^{1}$	0.29876×10^{1}
20	2·99093	$0{\cdot}28906 \times 10^{-3}$	$0{\cdot}55792 \times 10^{1}$	$0{\cdot}35671 \times 10^{1}$

Units $\partial h/\partial \varepsilon_1$: no dimension, $\partial Vs_i/\partial \varepsilon_1$: (m/s)

Table IV. Estimates from the sensitivities and the identified results (Type 2 function)

	Noise: 5%			Noise: 10%			Noise: 20%		
		Identified			Identified			Identified	
Parameter	Estimated	1st iterative value	Converged value	Estimated	1st iterative value	Converged value	Estimated	1st iterative value	Converged value
h	0·0604	0·0604	0·0586	0·0579	0·0579	0·0568	0·0509	0·0509	0·0499
Vs_1 (m/s)	201·32	201·32	202·05	205·64	205·64	205·73	216·69	216·69	218·05
Vs_2 (m/s)	502·96	503·96	502·60	506·73	506·73	506·73	510·67	510·67	510·65

Table V. Basic information on earthquake records

			Max. acc. at surface (gal)		
Marks	Origin time	M_{JMA}	EW	NS	Note
M	87·12·17 11:08:16	6·7	213·6	327·1	Main shock
A1	87·12·17 11:15:11	4·6	17·2	21·2	Aftershock
A2	87·12·17 14:07:06	4·4	23·8	13·8	Aftershock
A3	87·12·17 15:29:56	4·0	22·5	30·4	Aftershock
A4	88·01·05 10:09:02	4·2	40·6	40·8	Aftershock
A5	88·01·16 20:42:11	5·2	54·9	97·8	Aftershock

M_{JMA}: means Japan Meteorological Agency Magnitude

components: NS, EW, and UD. In this study, only the EW component was used for the observation data. This earthquake was strong with a maximum acceleration more than 200 gal. The aftershocks were not very strong, with acceleration below 60 gal. First, an optimum model in the linear range was identified using the average spectral ratios in the aftershocks, because the difference of strain level was shown between the main shock and the aftershocks clearly. Second, the effect of non-linear soil characteristics was estimated from the sensitivity of unknown parameters with respect to the difference in these transfer functions as measurement error. The soil characteristics were identified from the earthquake records and compared with the estimation from the sensitivities. Figure 6 shows the soil profile and the position of each seismometer. In this figure, the S-wave velocity indicate the PS logging data. The unit weight was the value assumed from the soil type.[17]

The principal motion was picked up by the measured data and the duration was set to 20·48 s. The ground level at -40 m was taken at the base level. Figure 7 shows the Fourier spectral ratio between seismometers at each level and GL $= -40$ m. In this figure, the thin solid lines indicate the average spectral ratio for the aftershocks, the dotted lines indicate the average value $\pm 1\sigma$, and the thick solid lines indicate the spectral ratio for the main shock. The Fourier spectral ratios for each aftershock were smoothed by 0·2 Hz Parzen window, then averaged. The Fourier spectral ratios for the main shock were smoothed by 0·5 Hz Parzen window. The latter window's band width was larger so that the smoothening degree for the main shock might match the apparent degree enhanced by the averaging of data from five aftershocks. The main shock and aftershocks exhibit clear primary, secondary, and tertiary peaks. Peaks in each of the main shock's spectral ratio shifted toward the lower frequency, compared with those of the aftershocks. This indicates a reduction in apparent shear modulus due to the non-linearity.

The unknown parameters in the identification problem were the S-wave velocity of each layer and common damping factor for the layers. The unit weight of each layer is known as shown in Figure 6. The analytical model consisted of 30 sub-layer elements, as shown in Figure 6, as a way of attaining sufficient accuracy in calculation at higher modes. Table VI shows the identified results obtained by the Type 1 and Type 2 evaluation functions, which used the average spectral ratio for the aftershocks. In this analysis, initial values are determined considering the PS logging data, the weight coefficients were taken as the inverse of the

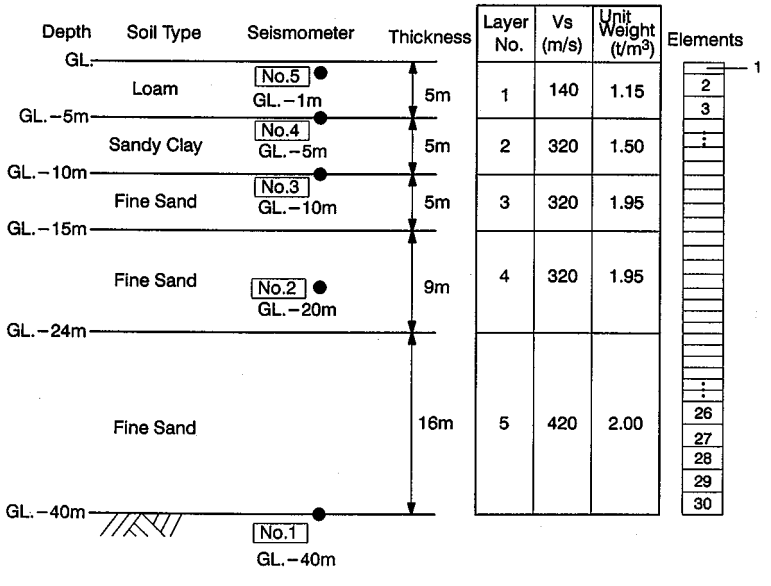

Figure 6. Soil profile and position of seismometers

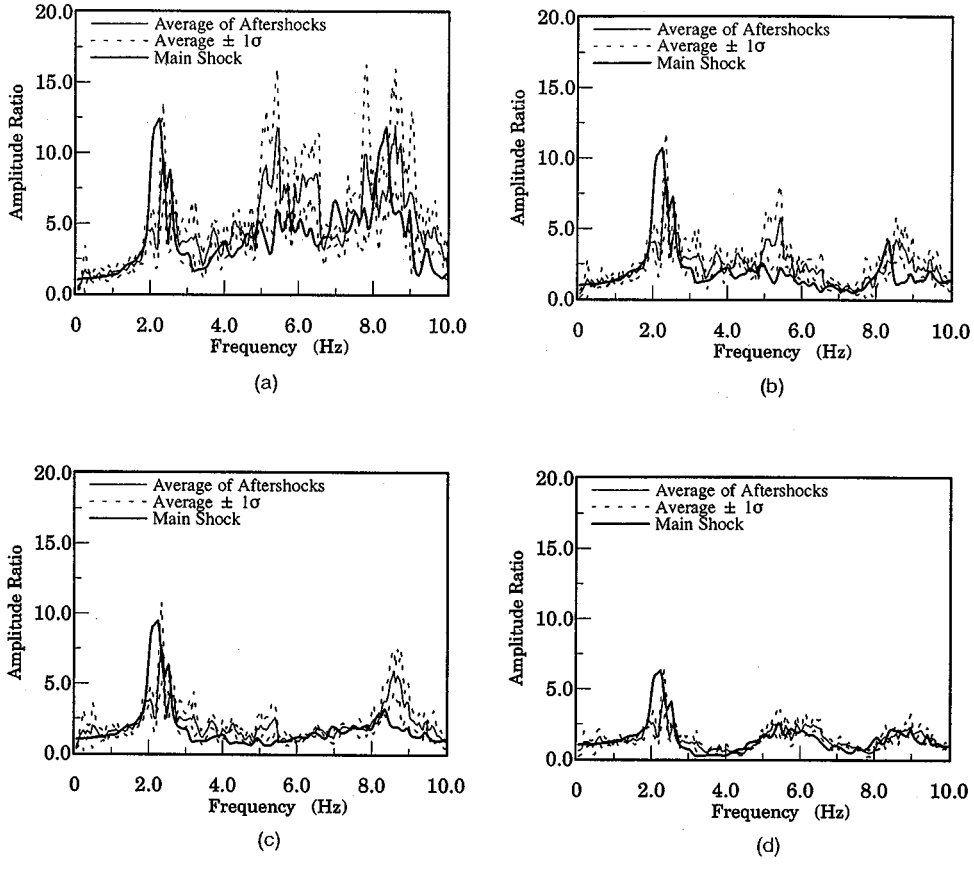

Figure 7. Fourier spectral ratio of earthquake records

Table VI. Identified results during the average spectral ratio for the aftershocks

Parameters	PS logging data	Identified	
		Type 1 function	Type 2 function
h	–	0·064	0·062
Vs_1 (m/s)	140	133·80	130·90
Vs_2 (m/s)	320	276·50	267·40
Vs_3 (m/s)	320	230·10	239·80
Vs_4 (m/s)	320	341·10	340·30
Vs_5 (m/s)	420	363·00	375·70

spectral ratio's variance for aftershocks. The range of frequencies was chosen from 1 to 10 Hz, where the SN ratios were good. No significant difference existed in the results between the Type 1 and Type 2 functions. At Layers 2, 3, and 5, the values identified from the evaluation functions deviated significantly from the PS logging data. As shown in Figure 8, the transfer function calculated from the results in Table VI agreed better

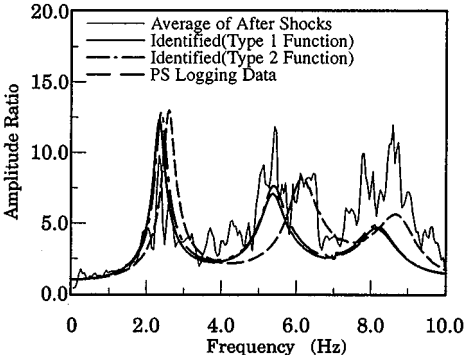

Figure 8. Comparison of identified results and observation data (GL. − 1 m/GL. − 40 m)

with the measured Fourier spectral ratio than the function calculated from the PS logging data. When calculating the transfer function from the PS logging data, the damping factor was taken to be 0·06 for all layers.

The difference between the transfer function obtained from the average spectral ratio of the aftershocks and the spectral ratio of the main shock may have been due to a measurement error. Therefore, the theory described in Section 3 was applied to estimate the effects of non-linearity and the identified values by using the spectral ratio of the main shock. The difference between the Fourier spectral ratio of main shock and the transfer function obtained from the average spectral ratio of the aftershocks is due to non-linearities. This disagreement arises from model error. However behaviour of non-linear system is often modeled by an equivalent linear system for the sake of simplicity. Then non-linearities are observed in the form of stiffness reduction and damping increase. In this chapter, equivalent damping and stiffness are estimated using information on the sensitivity analysis and the model identified from the average spectral ratio of the aftershocks. Table VII shows the calculated sensitivities of the parameters to observation error using the Type 1 evaluation function of equation (14). Table VIII shows those by using the Type 2 evaluation function of equation (15). In these tables, ℓ represents a combination of spectral ratios: $\ell = 1$ for GL-1 m/GL-40 m; $\ell = 2$ for GL-5 m/GL-40 m; $\ell = 3$ for GL-10 m/GL-40 m; and $\ell = 4$ for GL-20 m/GL-40 m. The weight coefficients were the inverse of the spectral ratio's variation for the aftershocks. In Tables VII and VIII, the negative sensitivities of the S-wave velocity were large at the first and the second layer. This fact would probably lead to a reduction of the shear modulus in near surface by non-linearity caused by strong motion. In lower layers, the positive and negative sensitivities were nearly equal in magnitude. This indicates that the identified results from the data of aftershocks might produce small fluctuations. The damping factors differed largely between the Type 1 and Type 2 functions. The Type 1 evaluation function lead the identified parameters obtained from the data of aftershocks to a negative fluctuation. On the other hand, the Type 2 evaluation function lead to a positive fluctuation.

Table IX shows those values of $(\bar{\mathbf{X}} + \sum_{i \in A} (\partial \mathbf{X}/\partial \varepsilon_i)\, \varepsilon_i)$ for the main shock estimated using the sensitivities with respect to measurement noise shown in Table VII which was calculated by the Type 1 evaluation function. This table also shows two types of identified results from the data on the main shock: first iterative value and final convergent value. The estimated value from sensitivities agreed perfectly with the first iterative value for each layer. The estimation differed from the convergent value presumably because of non-linearity between measurement noise and identified parameters.

Table X shows those values for the main shock estimated using the sensitivities with respect to measurement noise shown in Table VIII which was calculated by Type 2 evaluation function. This table also shows identified results from the data on the main shock. The estimated value from sensitivities agreed perfectly

Table VII. Sensitivities of unknown parameters with respect to measurement noise (Type 1 function)

ℓ	ε_ℓ	$\frac{\partial h}{\partial \varepsilon_\ell}$	$\frac{\partial Vs_1}{\partial \varepsilon_\ell}$	$\frac{\partial Vs_2}{\partial \varepsilon_\ell}$	$\frac{\partial Vs_3}{\partial \varepsilon_\ell}$	$\frac{\partial Vs_4}{\partial \varepsilon_\ell}$	$\frac{\partial Vs_5}{\partial \varepsilon_\ell}$
1	7·52189	$-0{\cdot}10215\times10^{-2}$	$0{\cdot}61692\times10^{0}$	$0{\cdot}17850\times10^{0}$	$-0{\cdot}62647\times10^{0}$	$-0{\cdot}19958\times10^{1}$	$0{\cdot}51874\times10^{0}$
2	4·55285	$-0{\cdot}77367\times10^{-3}$	$-0{\cdot}29920\times10^{0}$	$-0{\cdot}28951\times10^{0}$	$0{\cdot}10717\times10^{1}$	$0{\cdot}94348\times10^{0}$	-0.13697×10^{1}
3	3·90933	$-0{\cdot}14162\times10^{-3}$	$-0{\cdot}13360\times10^{1}$	$-0{\cdot}44534\times10^{1}$	$0{\cdot}42777\times10^{1}$	$0{\cdot}38396\times10^{1}$	$-0{\cdot}28641\times10^{1}$
4	2·25489	$0{\cdot}51368\times10^{-3}$	$-0{\cdot}52824\times10^{0}$	$0{\cdot}63190\times10^{0}$	$-0{\cdot}64421\times10^{1}$	$-0{\cdot}10146\times10^{2}$	$0{\cdot}51019\times10^{1}$

Units $\partial h/\partial \varepsilon_\ell$: no dimension, $\partial V_{si}/\partial \varepsilon_\ell$: (m/s)

Table VIII. Sensitivities of unknown parameters with respect to measurement noise (Type 2 function)

ℓ	ε_ℓ	$\frac{\partial h}{\partial \varepsilon_\ell}$	$\frac{\partial Vs_1}{\partial \varepsilon_\ell}$	$\frac{\partial Vs_2}{\partial \varepsilon_\ell}$	$\frac{\partial Vs_3}{\partial \varepsilon_\ell}$	$\frac{\partial Vs_4}{\partial \varepsilon_\ell}$	$\frac{\partial Vs_5}{\partial \varepsilon_\ell}$
1	0·9631943	$-0{\cdot}11608\times10^{-2}$	$0{\cdot}52164\times10^{0}$	$0{\cdot}52485\times10^{0}$	$-0{\cdot}86497\times10^{0}$	$0{\cdot}19927\times10^{1}$	$0{\cdot}48770\times10^{0}$
2	1·18782	$0{\cdot}30832\times10^{-2}$	$0{\cdot}22346\times10^{1}$	$0{\cdot}11838\times10^{1}$	$-0{\cdot}15133\times10^{1}$	$-0{\cdot}72555\times10^{1}$	0.60709×10^{1}
3	0·7928957	$0{\cdot}37897\times10^{-2}$	$-0{\cdot}85871\times10^{1}$	$-0{\cdot}13534\times10^{2}$	$0{\cdot}16953\times10^{2}$	$0{\cdot}12196\times10^{2}$	$0{\cdot}89041\times10^{1}$
4	1·12972	$0{\cdot}12693\times10^{-1}$	$-0{\cdot}49344\times10^{0}$	$0{\cdot}89763\times10^{0}$	$-0{\cdot}16119\times10^{2}$	$-0{\cdot}33138\times10^{2}$	$0{\cdot}12798\times10^{2}$

Units $\partial h/\partial \varepsilon_\ell$: no dimension, $\partial V_{si}/\partial \varepsilon_\ell$: (m/s)

Table IX. Estimates from the sensitivities and the identified results (Type 1 function)

Parameters	Estimated	Identified	
		1st iterative value	Converged value
h	0·0534	0·0534	0·0607
Vs_1 (m/s)	130·66	130·66	134·30
Vs_2 (m/s)	260·54	260·54	258·19
Vs_3 (m/s)	232·46	232·46	228·79
Vs_4 (m/s)	323·32	323·32	294·93
Vs_5 (m/s)	360·97	360·97	368·98

Table X. Estimates from the sensitivities and the identified results (Type 2 function)

Parameters	Estimated	Identified	
		1st iterative value	Converged value
h	0·0819	0·0819	0·0640
Vs_1 (m/s)	126·69	126·69	132·46
Vs_2 (m/s)	259·59	259·60	255·07
Vs_3 (m/s)	232·40	232·40	231·95
Vs_4 (m/s)	302·00	302·00	287·77
Vs_5 (m/s)	404·90	404·90	407·61

with the first iterative value for each layer. The estimation of the S-wave velocity was close to the convergent value. The damping factor was slightly different between the estimation and final convergence. Here, the estimation was a superposition of the product of the sensitivity and the remainder obtained for each of the four measured spectral ratios. Since this estimation was in perfect agreement with the first iterative value and in close agreement with the final convergent value, the present theory may be reasonable. Furthermore, calculated sensitivities of unknown parameters with respect to measurement noise were useful in estimating the effects of the soil's non-linearity.

5. CONCLUSIONS

This paper dealt with the effect of measurement noise on identification problems of soil characteristics from vertical array observation data. A method which evaluates the effect of measurement noise in terms of sensitivity was proposed. This method used either one of two theoretical evaluations functions: Type 1(anti-logarithmic) and Type 2(logarithmic). Numerical analyses were carried out to confirm the validity of the present theory. Furthermore, the present theory was applied to identify soil characteristics from actual earthquake records obtained by vertical array system. The conclusions obtained in this study are as follows:

(1) An equation for obtaining the sensitivity of an unknown parameter with respect to measurement noise was derived in the identification problems of the dynamic soil properties. A numerical simulation revealed that the obtained sensitivity was sufficiently accurate.

(2) The dynamic properties estimated by the sensitivity analysis agreed with the first iterative values of identification analysis.
(3) When using the Type 1(anti-logarithmic) evaluation function, the observation error had only a very small effect on the identified parameters. When using the Type 2(logarithmic) evaluation function, however, the observation error sometimes had a significant effect on the identified parameters. On the other hand, the sensitivities of unknown parameters with respect to measurement noise found to be calculated more accurately under the influence of large noises when using the Type 2(logarithmic) evaluation function.
(4) The present theory proved to be applicable to actual earthquake records even when measurement error exists at a number of observation points.
(5) When there is non-linearity in the soil characteristics which could be caused by strong motions, the sensitivities obtained from the remainder of a spectral ratio proved to be useful for evaluating reduction in shear modulus of the soil in near-surface layer.

ACKNOWLEDGEMENTS

The authors would like to thank Professor T. Katayma of Institute of Industrial Science, University of Tokyo, for allowing us to use the vertical array records in this study.

REFERENCES

1. T. Annaka, T. Tsuzuki, T. Masuda, M. Shimada and K. Okadome, 'Strain dependence of shear modulus and damping factor of soil deposit inferred from the strong motion accelerograms record by a vertical array', *Proc. 9th Japan earthquake engineering symp.* Vol. 1, December 1994, pp. 493–498 (in Japanese).
2. T. Suzuki and M. Tanaka, 'An approach to evaluate microtremor data based on the result of identification analysis for S-wave velocity profile of surface soil deposits', *Proc. 9th Japan earthquake engineering symp.*, Vol. 1, December 1994, pp. 217–222 (in Japanese).
3. Y. Okamoto, T. Sawada, K. Hirao and O. Tsujihara, 'Localized identification of S-wave velocity and quality factor of surface layers by using vertical array records', *Proc. 9th Japan earthquake engineering symp.*, Vol. 1, December 1994, pp. 289–294 (in Japanese).
4. T. Sato, H. Kawase and T. Sato, 'Engineering bedrock wave obtained through the identification analysis based on borehole records and their statical envelope characteristics', *J. struct. construction eng.* **461**, 19–28 (1994) (in Japanese).
5. T. Sato, H. Kawase and T. Sato, 'Statistical spectral characteristics for engineering bedrock waves in which local site effects of surface geology are removed', *J. struct. construction eng.* **462**, 79–89 (1994) (in Japanese).
6. T. Kurita and I. Yoshida, 'Identification of soil properties from the records of 1987 Chibaken-Toho-Oki earthquake and its after shocks', *Proc. 49th Annual Conf. of the Japan society of civil engineers*, Vol. 1(A), September 1994, pp. 1524–1525 (in Japanese).
7. T. Sawada, O. Tsujihara, H. Asega and H. Kamiya, 'A few remarks on the identification of linear chain model with multi-degrees of freedom in the frequency domain', *J. struct. eng.* **32A**, 739–748 (1986) (in Japanese).
8. G. H. McVerry, 'Structural identification in the frequency domain from earthquake records', *Earthquake eng. struct. dyn.* **8**, 161–180 (1980).
9. K. Matsui and T. Kurita, 'Structural identification from input and output acceleration records', *J. Struct. Engng.* **35A**, 689–698 (1989) (in Japanese).
10. T. Kurita and K. Matsui, 'Comparative study on application of dynamic programming and Gauss-Newton method to structural identification problem', *Proc. Symp. on computational methods in structural engineering and related field*, Vol. 13, July 1989, pp. 413–418 (in Japanese).
11. K. Matsui and T. Kurita, 'Sensitivities of parameters due to model errors and measurement noises in structural identification problems', *Proc. JSCE, structural engineering/earthquake engineering*, No. 422/I-14, October 1990, pp. 145–154.
12. P. C. Shah, 'A methodology for optimal sensor location of dynamic systems', *Trans. ASME, J. appl. mech.* **45**, 188–196 (1978).
13. O. Tsujihara, T. Sawada and K. Hirao, 'Comparison of some nonlinear programming algorithms in identification of dynamic soil properties', *J. struct. mech. earthquake eng. JSCE* **489/I-27**, 277–280 (1994) (in Japanese).
14. I. Yoshida, K. Toyoda and M. Hoshiya, 'Formulation and solver for probablistic back analysis with 2-D FEM', *J. struct. mech. earthquake eng. JSCE* **507/I-30**, 129–136 (1995) (in Japanese).
15. I. Yoshida, H. Kurose and S. Fukui, 'Basic study on probabilistic back analysis', *J. struct. mech. earthquake eng. JSCE* **483/I-26**, 61–68 (1994) (in Japanese).
16. T. Nakagawa and Y. Oyanagi, *Least square method for experimental data analysis*', University of Tokyo Press, Tokyo, 1982 (in Japanese).
17. T. Katayama, F. Yamazaki, S. Nagata, L. Lu and T. Turker, 'A strong motion database for the Chiba seismometer array and its engineering analysis', *Earthquake eng. struct. dyn.* **19**, 1089–1106 (1990).

